Contrib Mineral Petrol (1990) 105:650–661

Contributions to Mineralogy and Petrology

Meta-igneous granulite xenoliths from Mount Ruapehu, New Zealand: fragments of altered oceanic crust?

Ian J. Graham[1], **Peter Blattner**[1,2], **and Malcolm T. McCulloch**[3]

[1] Institute of Nuclear Sciences, Lower Hutt, New Zealand
[2] New Zealand Geological Survey, Lower Hutt, New Zealand
[3] Research School of Earth Sciences, Australian National University, Canberra, Australia

Received January 11, 1989 / Accepted April 20, 1990

Abstract. Meta-igneous granulite (MIG) xenoliths in lavas from Mount Ruapehu, Taupo Volcanic Zone, New Zealand, have variable but relatively high $\delta^{18}O$ (+8.2 to +11.7) and $^{87}Sr/^{86}Sr$ (0.70506 to 0.70872), and ε_{Nd} ranging from +1.5 to +6.2. They show a strong positive correlation between $^{87}Sr/^{86}Sr$ and $\delta^{18}O$, both of which are also broadly correlated with Mg number, but lack any correlation between $^{87}Sr/^{86}Sr$ and ε_{Nd}. The xenoliths have been mineralogically re-equilibrated at lower-crustal temperatures (800–930° C) and pressures (7–10 kbar). Geochemical and isotopic evidence suggests they are fragments of oceanic crust that have been altered previously in an ocean floor hydrothermal system. Alternatively, they may be igneous rocks of unknown origin hydrothermally altered in the lower crust. Irrespective of this uncertainty, the xenoliths provide rare samples of the lower crustal basement beneath Taupo Volcanic Zone and represent a potential source rock for the voluminous rhyolites and ignimbrites that dominate the zone.

Introduction

The Taupo Volcanic Zone (TVZ) is the southward extension of the Tonga Kermadec Arc into the continental crustal environment of New Zealand (Fig. 1). Westwards dipping, oblique subduction of the Pacific plate beneath the Indian Plate (Fig. 1, inset) has produced a young (<250 ka) andesite-dacite volcanic arc (Taupo Arc) extending along the eastern side of the zone. A 50-km-wide volcanotectonic depression (marginal basin?; Cole and Lewis 1981) extends up to 50 km westwards of the central part of the arc and comprises a series of rhyolitic centres (Cole 1979).

A continuing puzzle confronting New Zealand volcanology is the origin of the voluminous rhyolitic magmas that dominate the TVZ. Past theories involving melting of exposed Mesozoic greywacke-argillite (Cole 1979; Reid 1983) have been largely refuted by isotopic data (Blattner and Reid 1982) and on experimental grounds (Conrad et al. 1988). As a consequence, current research is concentrated on a possible lower crustal source.

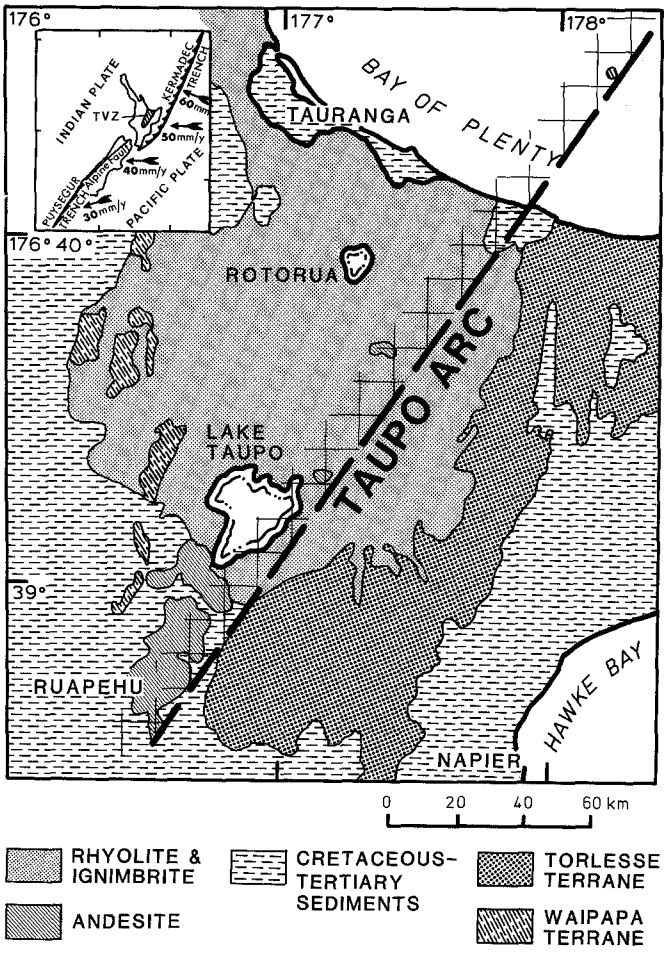

Fig. 1. Taupo Volcanic Zone (*TVZ*) showing the location of the Taupo Arc and distribution of basement lithologies. *Inset* shows the tectonic setting of the TVZ and the nature of the Pacific-Indian plate boundary in the New Zaland region

Offprint requests to: I.J. Graham

In this paper we report petrographic, geochemical and isotopic data for a suite of meta-igneous granulite (MIG) xenoliths from Mt. Ruapehu, in the southern part of the Taupo Arc (Fig. 1). These xenoliths were clearly equilibrated at temperatures consistent with a lower arc-crust origin and thus provide a unique window into the lower crust beneath the TVZ. It is now widely recognised that island arc magmatism plays a crucial role in the growth and development of continental crust throughout the Phanerozoic and possibly the Precambrian. Whilst there have been numerous studies of arc magmas [see Arculus (1986) and Gill (1981) for recent reviews], questions relating to the nature and origin of the lower arc-crust remain. For example, does it consist predominantly of cumulates produced by crystal fractionation of arc magmas (cf. Conrad and Kay 1984; Hildreth and Moorbath 1988) or residues resulting from partial melting of oceanic crust (Kay and Kay 1986; Ruiz et al. 1988)? This paper seeks to address some of these questions, particularly in relation to the Taupo Arc.

General description of MIG xenoliths

Distinguishing characteristics

Table 1 presents a summary of all xenolith types found in Ruapehu lavas. MIG xenoliths make up about 20% of the *metamorphic* xenoliths recovered and form a distinct group based on mineralogy, bulk-rock chemistry and isotopic composition. Most of the remaining metamorphic xenoliths have been interpreted to be restites after partial melting of Torlesse terrain greywacke (Graham 1987), which comprises the dominant known basement rock of the eastern North Island of New Zealand (Fig. 1). Like MIG xenoliths, these have refractory assemblages and high-grade metamorphic textures, indicating regional pyroxene-hornfels or granulite facies conditions (Winkler 1979). However, they have demonstrably different mineralogies (Table 1) and chemical compositions (Graham 1987), making them easily distinguishable as a separate group.

In addition to the wide range of metamorphic xenoliths, there is an abundance of *igneous* types ranging from volcanics to cognate cumulates (Graham and Hackett 1987). Glomerocrysts of a few millimeter in diameter are also common in many lavas. Most of these are fragments of larger nodules with mineral compositions similar to host lava phenocrysts whereas others are more ultramafic in composition and are probably mantle-derived. Some are not clearly cognate and may be related to an earlier magma with a contact metamorphic overprint reflecting a time-gap between formation and incorporation; textural criteria alone are insufficient to distinguish these from MIG xenoliths but mineralogy, chemical and isotopic compositions are usually decisive.

Petrography

MIG xenoliths are typically small (<300 nm), grey and fine-grained (<2–5 mm; Fig. 2). Although there is considerable textural diversity, all examples show evidence of metamorphism ranging from partial overprinting of recognisable cumulate textures to complete textural re-equilibration (cf. Dostal et al. 1980). Coarser-grained examples are poikiloblastic and sometimes show a directional fabric representing relict layering or possibly a later schistosity (Fig. 2A). Others (e.g. 17414) are cataclastic due to severe shearing stress prior to inclusion in the host lava. Finer-grained examples are mostly xenomorphic granular (Fig. 2B), and a few (e.g. 17450) have porphyroblastic textures. Xenolith-host contacts are usually sharp and regular, although some show evidence of mineralogical reaction involving preferential growth of plagioclase on the host side (Fig. 2C).

Mineral assemblages are anhydrous and are restricted in most cases to plagioclase, orthopyroxene, clinopyroxene and ilmenite. Chrome spinel occurs in two examples (17414, 17442) and quartz becomes more dominant as bulk-rock silica increases. Hornblende is absent. Small amounts of interstitial silica-rich glass (charged with microlites of pyroxene) occur in one example (17422) (Fig. 2D). Minerals show at best only poorly developed chemical zonation (Table 2); plagioclase ranges in composition from An_{46} (17422) to An_{88} (17424), and is low in potassium (typically ≤ 2 mol% Or); orthopyroxene is bronzite to hypersthene and compositions are relatively Ca-poor compared with host lava phenocrysts (Fig. 3); clinopyroxenes are mainly augites containing less than 2 wt% Al_2O_3. Ilmenites are also low in alumina and contain 3–6 wt% MgO. Chrome spinel has high $Cr/(Cr+Al)$(78–79) and low $Mg(Mg+Fe^{2+})$(25–33).

Chemical composition

Bulk-rock chemical compositions of MIG xenoliths are broadly igneous in character but are widely variable (Ta-

Table 1. Summary of main xenolith types in Ruapehu lavas

Lithology	Relative abundance %	Mineralogy
Metamorphic xenoliths	(70)	
Porcellanite	Rare	Q + Pl + sintered matrix ± Cpx ± Zir
Buchitic metagreywacke	Rare	Glass + Q + Cor + Opx + Pleon + Il ± Rut ± Pyrr
Garnet-schist	1–2	Q + Pl + Cpx + Opx ± Gnt ± Mt ± Il ± Bi ± Glass
Metaquartzite	25	Q + Pl + Cpx ± Woll ± Opx ± Glass
Biotite-schist	1–2	Pl + Ks + Bi + Opx ± Q ± Sill ± Il ± Pleon ± Glass
Pyroxene-hornfels	25	Pl + Op + Mt + Il ± Pleon ± Co ± Glass
Spinel-schist	2–3	Pl + Bi + Opx + Mt + Il ± Ol ± Glass
Granulite (MIG)	15	Pl + Cpx + Opx + Il ± Cr-Sp ± Q ± Glass
Igneous xenoliths	(30)	
Volcanics	20	Pl + Cpx + Opx + Mt ± Ol
Cumulates	8	Pl + Cpx + Opx + Mt ± Ol
Ultramafics	2	Ol or Pl or Cpx + Pl or Cpx + Opx ± Cr-Sp ± Mt

Pl = plagioclase; Cpx = clinopyroxene; Opx = orthopyroxene; Gnt = garnet; Bi = biotite; Woll = wollastonite; Ks = alkali feldspar; Sill = sillimanite; Pleon = pleonaste; Ol = olivine; Cr-Sp = chrome spinel; Cor = cordierite; Rut = rutile; Pyrr = pyrrhotite; Zir = zircon; Q = quartz; Il = ilmenite; Mt = magnetite; Co = Corundum

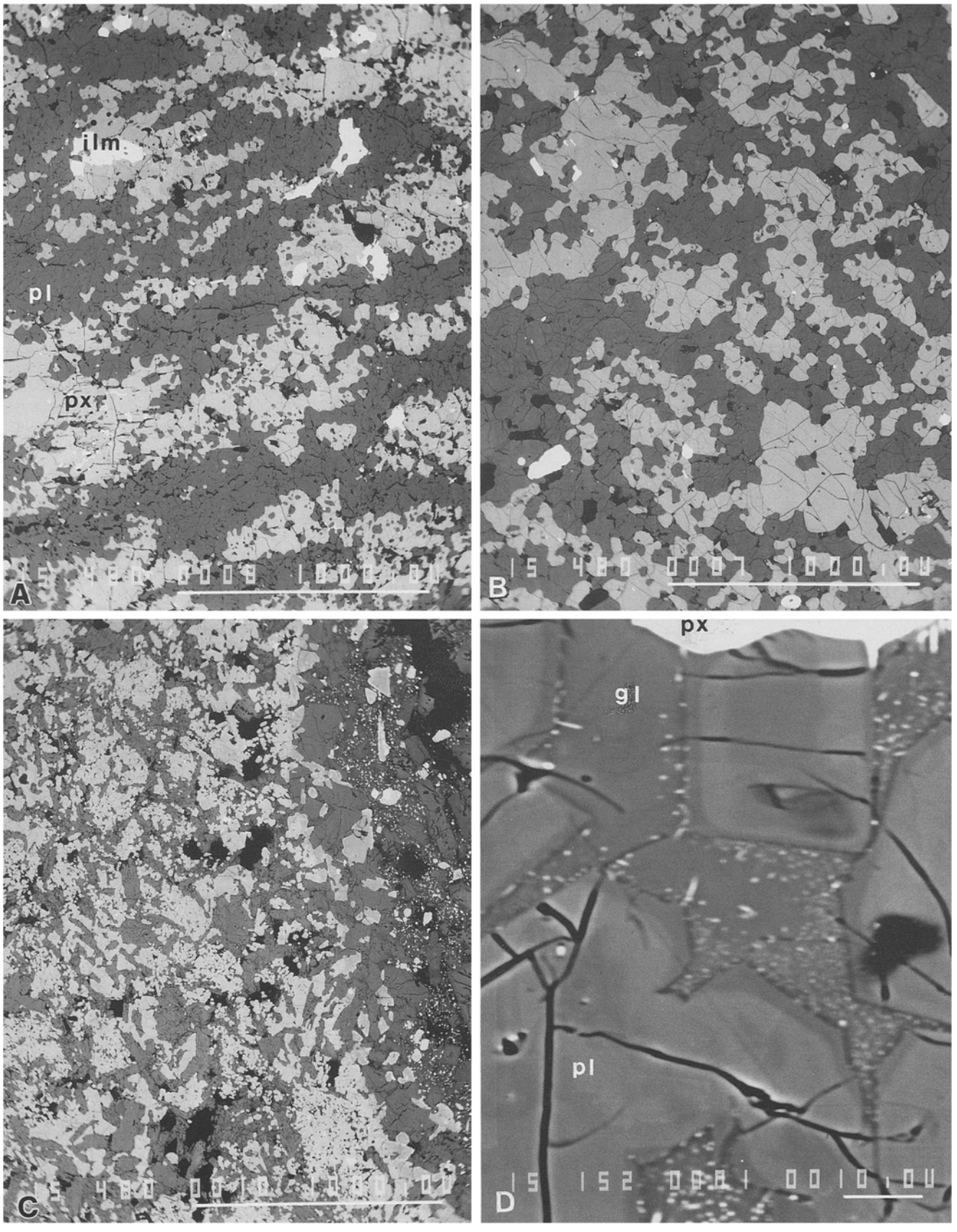

Fig. 2A–D. Back scattered electron image photographs of MIG xenoliths: **A** 17424 showing granoblastic texture with a strong directional orientation (grey = plagioclase; light grey = pyroxene; white = ilmenite; field of view 1.9 mm); **B** 17441 showing granoblastic texture with coarse poikiloblastic pyroxene (field of view 1.9 mm); **C** Contact between 17442 (right hand side) and host lava. Crystals on xenolith rim are in chemical equilibrium with host lava and have euhedral terminations (field of view 1.9 mm); **D** 17422 showing plagioclase (grey, euhedral crystals with Na-rich rims) in contact with rhyolitic glass ($SiO_2 = 76.8$ wt%; $TiO_2 = 0.9\%$; $Al_2O_3 = 12.4\%$; $FeO = 0.8\%$; $MgO = 0.1\%$, $CaO = 0.5\%$, $Na_2O = 2.6\%$; $K_2O = 5.9\%$) (field of view 0.06 mm)

Table 2. Compositions of minerals in MIG xenoliths

	Plagioclase			Orthopyroxene			Clinopyroxene			Ilmenite % Il	Equilibration Temperature (°C)	Other minerals present
	An	Ab	Or	Wo	En	Fs	Wo	En	Fs			
17414	55.3	42.9	1.8	2.1	66.8	31.1	42.8	46.4	10.8	96.0	860	Chrome spinel
17421	62.0	37.1	0.9	3.8	62.8	33.4	43.0	45.9	11.1	94.0	830	—
17422	46–53	52–45	2.0	3.1	57.0	39.9	39.5	41.2	19.3	—	910	Titanomagnetite, glass
17424	79–88	21–12	0.1	3.2	56.8	40.0	39.0	40.7	20.3	91.4	930	—
17432	67.4	31.0	1.6	1.6	56.3	42.1	—	—	—	—	—	Quartz
17433	79.8	19.7	0.5	2.0	52.8	45.2	41.0	39.9	19.1	93.1	835	Quartz
17441	62.1	36.6	1.3	2.6	67.0	30.4	43.5	44.0	12.5	92.0	795	—
17442	71.0	28.3	0.7	2.1	74.4	23.5	42.5	49.0	8.5	93.5	905	Chrome spinel
17449	50.8	45.9	3.3	1.6	65.7	32.7	42.5	41.5	16.0	99.6	800	Quartz
17450	57–89	41–10	2–1	1.1	53.0	45.9		—		95.5	—	Quartz

All mineral analyses made using Jeol 733 electron microprobe at Victoria University Analytical Facility (Wellington, New Zealand): Accelerating potential = 25 kV, specimen current = 1.2×10^{-8} A, beam diameter = 3 μm. Analytical precision = ± 2%.
Pyroxene endmembers calculated after the method of Lindsley (1983).
Equilibration temperatures (for clinopyroxene) determined graphically (Fig. 3):
Full chemical analyses are available from the authors on request

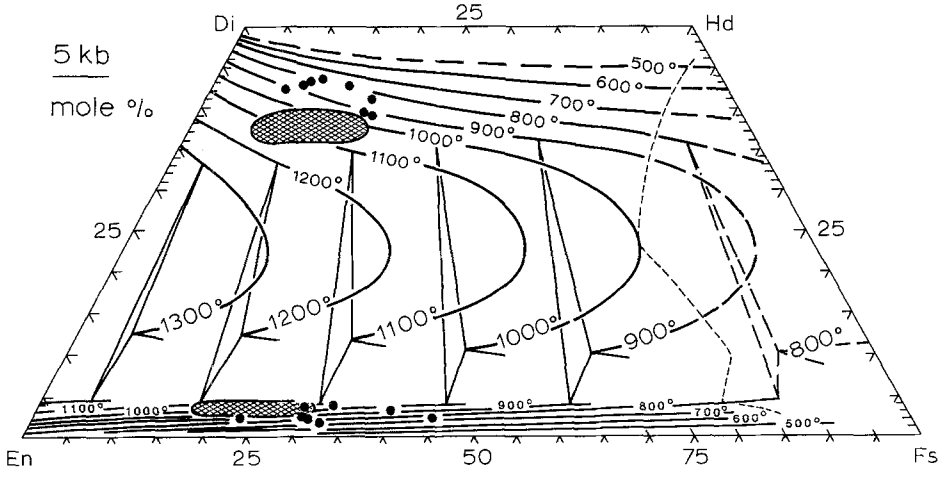

Fig. 3. Polythermal orthopyroxene-clinopyroxene-pigeonite plot for MIG xenoliths (Lindsley 1983). The fields of host lava pyroxene core compositions are *hashed*

ble 3), with SiO_2 ranging from 49 to 60 wt%, and Mg numbers ranging from 52 to 78. Oxidation ratios (Fe_2O_3/FeO) are close to 0.22 and water contents (LOI) average 0.96 weight %. All but one of the xenoliths are quartz normative and the three most silica-rich examples are slightly corundum-normative. Most compositions are tholeiitic, with low alkali contents and relatively high FeO contents. The observed wide variations in Al_2O_3 and MgO contents presumably reflect original feldspar: mafic mineral ratios. This is supported by tight correlations between Mg number and Cr or Ni (Fig. 4), controlled mainly by original olivine content. On the basis of Cr and Ni contents, some 60% of MIG xenoliths must originally have contained olivine, which reacted out during metamorphic re-equilibration. The Mg number also seems well correlated with the grain size.

All xenoliths have trace element patterns similar to volcanic arc magmas showing LILE-enrichment and HFSE/HREE depletion, when compared with N-MORB (Fig. 5). Most compositions, however, show only moderate enrichment in LILE (75% lie between 17441 and 17449 on Fig. 5) whilst two show unusually high enrichment (17432 and 17414) and two unusually low (17433 and 17424). Low concentrations of Rb relative to Zr (Rb/Zr = 0.030 to 0.915; Table 3) occur for all but two of the xenoliths. This feature has been described for granulites elsewhere (e.g. Rudnick et al. 1985), and may suggest syn-metamorphic depletion (by partial melting?) of mobile, LILE elements from within the xenolith protolith.

On a Ti versus Zr diagram (Fig. 6), compositions fall into an intermediate field between arc tholeiite and calc-alkaline rocks. The danger of extrapolating this diagram to high-grade metamorphic rocks is acknowledged: it is not known whether these elements have mobilised under high P-T conditions. However, almost all of the MIG xenolith compositions plot in a tight bunch which, considering the wide variations in major and trace element chemistry, suggests only minor relative mobility (note that 17424 and 17430 have high Ti contents due to localised high abundance of ilmenite).

Isotopic compositions

Sr, Nd and oxygen isotopic analyses of a selection of MIG xenoliths are presented in Table 3 and illustrated

Table 3. Bulk-rock chemistry of Ruapehu granulite xenoliths

Cat	17430	17424	17479	17441	17411	17494	17442	17421	17431	17414	17422	17449	17433	17432	17450	17495
analysis no	1	2	3	4	5	6	7	8	9	10	11	12	13	14	15	16
SiO_2	48.5	48.8	50.8	52.6	52.6	52.9	53.4	53.7	54.5	55.0	55.1	57.3	57.6	58.9	60.2	60.3
TiO_2	1.36	1.50	0.72	0.62	0.57	0.69	0.55	0.52	0.59	0.50	0.69	0.64	0.55	0.61	0.65	0.62
Al_2O_3	18.2	16.9	19.7	15.3	13.2	14.4	13.8	15.2	19.3	13.7	17.2	14.8	17.1	19.0	18.6	18.0
Fe_2O_3	1.5	2.2	1.6	1.6	1.6	1.5	1.4	1.4	1.4	1.3	1.4	1.3	1.3	1.2	1.2	1.3
FeO	7.7	10.8	8.2	7.8	7.8	7.4	6.9	6.9	7.2	6.7	6.7	6.5	6.5	5.9	5.7	6.2
MnO	0.13	0.29	0.21	0.19	0.15	0.15	0.14	0.19	0.12	0.12	0.17	0.16	0.15	0.10	0.14	0.11
MgO	6.7	8.7	8.0	9.7	14.2	10.6	12.9	10.3	5.6	13.1	5.1	7.9	5.4	3.9	3.5	3.9
CaO	13.4	9.3	7.9	10.0	8.1	9.9	8.9	8.9	7.3	6.8	9.2	8.5	10.1	7.5	7.6	6.7
Na_2O	2.0	1.5	2.4	1.8	1.7	2.2	1.6	2.6	3.4	1.8	3.6	2.6	1.2	2.3	2.1	2.6
K_2O	0.23	0.10	0.27	0.26	0.13	0.22	0.34	0.26	0.54	0.76	0.66	0.38	0.09	0.50	0.22	0.23
P_2O_5	0.18	0.05	0.09	0.06	0.08	0.08	0.09	0.08	0.13	0.04	0.11	0.06	0.09	0.10	0.10	0.03
LOI	1.4	1.4	0.4	0.2	1.8	0.4	0.2	0.9	0.7	1.9	1.0	0.4	1.2	1.8	0.8	1.2
(Total)	100.45	100.06	98.88	100.28	99.83	99.24	99.99	100.77	99.57	100.12	100.14	99.58	100.0	100.2	99.6	99.8
Q	0.0	1.2	1.6	3.2	1.1	1.5	2.8	1.7	4.2	4.5	3.3	9.6	18.0	18.2	21.9	19.6
Co	0.0	0.0	1.5	0.0	0.0	0.0	0.0	0.0	0.2	0.0	0.0	0.0	0.0	1.5	1.4	1.4
Or	1.4	0.6	1.6	1.6	0.8	1.3	2.0	1.6	3.2	4.6	4.0	2.3	0.5	3.0	1.3	1.4
Ab	17.2	12.6	19.9	15.3	14.2	18.5	13.6	21.7	28.5	15.6	30.6	21.8	10.5	19.0	17.7	22.3
An	39.9	39.1	38.5	33.0	28.1	28.8	29.5	29.0	35.3	27.2	28.7	27.6	40.7	36.3	37.0	32.8
Di	20.7	5.5	0.0	13.4	9.2	16.0	11.2	11.6	0.0	5.3	13.5	11.3	7.0	0.0	0.0	0.0
Hy	10.5	34.9	32.9	30.0	43.2	30.2	37.6	31.2	25.1	40.0	16.5	24.2	20.2	18.9	17.6	19.4
Mt	2.2	3.1	2.4	2.3	2.3	2.2	2.0	2.0	2.1	1.8	2.0	1.9	1.9	1.7	1.7	1.8
Il	2.6	2.9	1.4	1.2	1.1	1.3	1.1	1.0	1.1	1.0	1.3	1.2	1.1	1.2	1.3	1.2
Ap	0.4	0.1	0.2	0.1	0.2	0.2	0.2	0.2	0.3	0.1	0.3	0.4	0.2	0.2	0.2	0.1
Mg-number	61	59	63	69	77	72	77	73	58	78	57	68	60	54	52	53
Oxid rat	0.51	0.16	–	–	0.18	–	–	0.13	0.25	0.13	0.34	–	0.08	0.23	–	–
Ba	125	71	280	107	146	110	132	129	173	141	97	163	54	353	90	228
Cr	268	242	311	445	1046	558	798	627	43	673	84	555	99	25	18	25
Cu	67	14	67	24	28	80	23	24	77	42	52	20	33	30	7	29
Ga	18	15	21	16	15	16	13	17	19	13	19	18	20	23	17	20
Nd	9.3	4.1	–	6.8	–	7.1	7.0	6.2	5.0	6.1	7.1	11.6	5.6	6.9	9.8	–
Ni	71	99	73	130	395	174	292	173	12	334	19	80	35	7	12	15
Pb	4	6	5	3	3	6	7	<2	6	9	9	8	6	12	8	11
Rb	6	2	5	6	4	5	10	4	16	43	17	9	2	55	6	2
Sc	48	40	32	31	36	36	31	26	20	31	27	28	24	21	21	24
Sm	2.7	1.2	–	1.9	–	2.0	1.8	1.7	1.2	1.7	1.9	2.7	1.7	1.8	2.5	–
Sr	373	210	392	249	186	242	300	230	379	329	412	368	194	809	245	259
V	273	374	232	244	196	266	204	199	182	182	245	222	201	197	207	204
Y	23	12	14	15	15	18	15	14	11	16	18	18	16	14	19	12
Zn	67	106	226	87	89	77	84	78	79	78	82	81	73	74	86	93
Zr	66	31	116	37	52	59	54	35	37	47	56	63	51	69	61	66
K/Rb	301	517	492	335	308	367	290	521	277	146	319	367	532	76	315	908
Rb/Zr	0.091	0.065	0.043	0.162	0.007	0.085	0.185	0.114	0.432	0.915	0.303	0.143	0.039	0.797	0.098	0.030
Rb/Sr	0.017	0.008	0.012	0.026	0.019	0.021	0.032	0.018	0.043	0.13	0.041	0.023	0.007	0.067	0.024	0.008
$^{87}Sr/^{86}Sr$	0.70670	0.70637	0.70600	0.70593	0.70642	0.70506	0.70570	0.70611	0.70594	0.70792	0.70648	0.70560	0.70689	0.70872	0.70679	0.70581
$^{143}Nd/^{144}Nd$	0.51285	0.51273	–	0.51278	–	0.51295	0.51289	0.51282	0.51290	0.51291	0.51291	0.51278	0.51296	0.51292	0.51281	–
$\delta^{18}O‰(SMOW)^a$	–	+9.5[2]	–	+9.1	–	+8.2	+8.5	–	–	+10.7	+10.3	+8.2[2]	+9.7	+11.7	+10.3	–

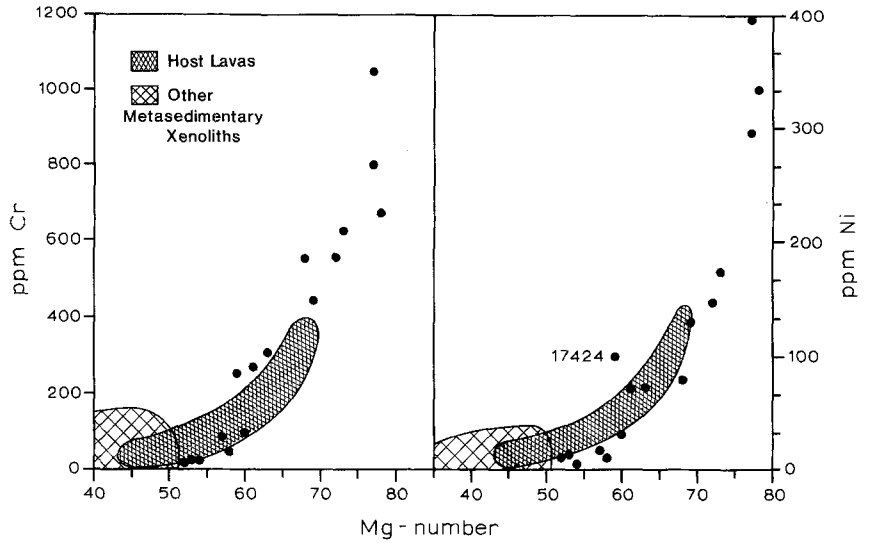

Fig. 4. Mg number vs Cr and Ni, showing a close similarity in trends between MIG xenoliths and host lavas, but much higher concentrations of Cr and Ni in many of the xenoliths. The field for other metasedimentary xenoliths (Torlesse derivatives, Graham 1987) is also given

in Figs. 7 to 9. Strontium isotope ratios are relatively high, despite low Rb/Sr, and range from 0.70506 to 0.70872. Model Rb-Sr ages using an assumed initial $^{87}Sr/^{86}Sr$ of 0.7045 are in the order of several hundred million years, much older than the presently known basement of the central North Island (140–200 Ma; Graham 1985), and as old or older than the oldest crystalline basement in New Zealand (~680 Ma; Adams 1975). Because of the diverse geochemistry of the xenoliths and probable selective loss of Rb during metamorphism, these ages are not considered to have any geological meaning. Nd isotopic ratios range from 0.51273 to 0.51296 and similarly scatter on an isochron diagram. Oxygen isotope ratios range from +8.2 to +11.7 and show a strong positive correlation with $^{87}Sr/^{86}Sr$ (Fig. 7), whereas there is no obvious correlation between $^{87}Sr/^{86}Sr$ and ε_{Nd} (Fig. 8). Both $\delta^{18}O$ and $^{87}Sr/^{86}Sr$ show a weak correlation with Mg number (Fig. 9). (Note that 17414 falls well to one side of this trend.)

P-T conditions of metamorphic re-equilibration

Bulk-rock chemical compositions of MIG xenoliths clearly require derivation from an original igneous protolith and high grade metamorphism appears to have strongly modified original textures and mineralogy. Al-

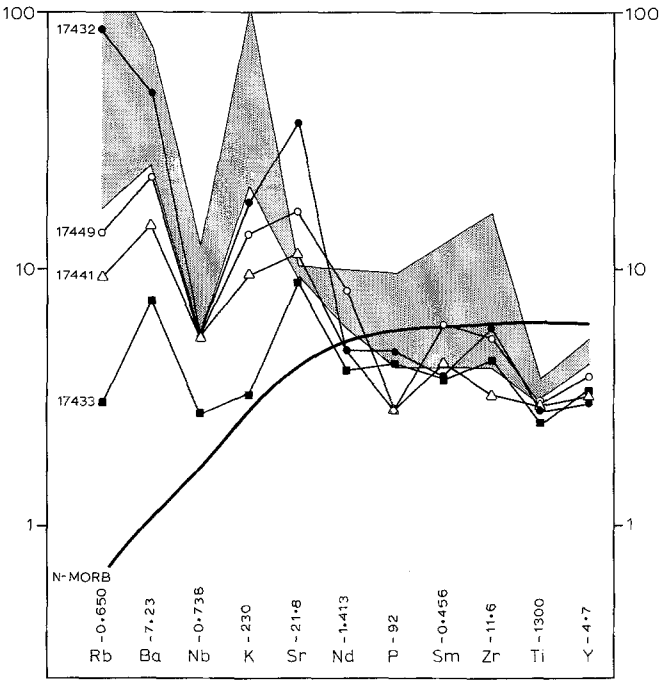

Fig. 5. Trace element contents of MIG xenoliths normalised against primitive mantle and ordered according to their ionic potential (Pearce 1982). For clarity a selection has been made from Table 3. Normalising constants and N-MORB values are from McDonough et al. (1985). Nb data are close to detection limit and are therefore given as maximum values (i.e. measured value +2 ppm). The field of host lava is *hashed*

Major element compositions determined using standard methods on a Siemens SRS-1 XRF at the Victoria University Analytical Facility (analytical precision = ±1% (2σ)). Analyses are normalised to 100% volatile-free (volatile loss (LOI) and original totals are given for comparison). Mg-number = 100 (Mg/(Mg+0.8 Fe^{2+})). Actual oxidation ratios (Fe_2O_3/FeO) are given for some samples. Di = Diopside, Hy = hypersthene, Ap = Apatite, (other abbreviations as for Table 1).

Trace element compositions determined by XRF (2σ precision typically ±2 ppm) except Nd and Sm by isotope dilution. " – " not determined

Sr analysed isotopically on a VG MM30B mass spectrometer at the Institute of Nuclear Sciences, Lower Hutt, New Zealand (Graham 1985, 1986). NBS987 = 0.71020; precision ≤0.00008 (2σ)

Nd analysed isotopically on a Finnigan MAT261 mass spectrometer at Australian National University, Canberra, Australia (McDonough et al. 1985). BCR-1 = 0.512654 ± 0.000005; precision ≤ ±0.000001 (2σ)

Oxygen analysed isotopically on a NAA6-60-RMS mass spectrometer at the Institute of Nuclear Sciences, Lower Hutt, New Zealand (see Blattner and Reid 1982) NBS28 = 9.60‰ (SMOW); precision <0.2‰ (1σ)

[a] Plagioclase = 10.1 ± 0.15‰ pyroxene = 9.1 ± 0.15‰ [2]plagioclase = 8.4 ± 0.2‰ pyroxene = 7.4 ± 0.1‰

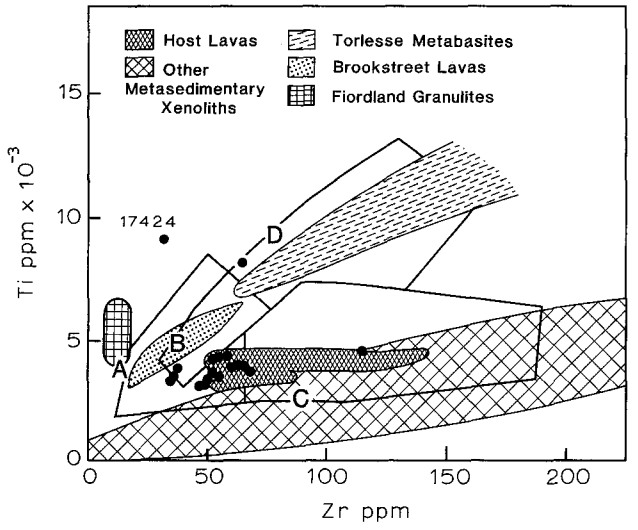

Fig. 6. Ti versus Zr diagram for MIG xenoliths showing distinctions between possible volcanic protoliths. Fields are as follows: low-K tholeiites = *A* and *B*; calc-alkaline basalts = *B* and *C*; ocean floor basalts = *B* and *D* (Pearce and Cann 1973). Torlesse metabasite compositions from Grapes and Palmer (1984) and Roser (1983), Brookstreet lava compositions from Sivell and Rankin (1983), Fiordland granulite compositions from Blattner (unpublished data), host lava compositions from Graham and Hackett (1987), and other metasedimentary xenolith compositions from Graham (1987)

though lack of suitable mineral assemblages make pressure estimates somewhat imprecise, the removal of olivine via the reaction olivine + plagioclase = orthopyroxene + clinopyroxene ± spinel ± plagioclase (Green and Ringwood 1967) indicates pressures greater than 7–9 kbar. On the other hand, the absence of garnet in any of the samples places an upper pressure limit of about 10 kbar (Green and Ringwood 1967). Crustal thickness estimates from recent geophysical (seismic and microearthquake) studies of the central North Island are about 30–35 km (Stern and Davey 1987; Reyners 1980), which would suggest that MIG xenoliths re-equilibrated in the lowermost crust beneath Ruapehu. Equilibration temperatures for coexisting pyroxenes, calculated after the method of Lindsley (1983), range between 795° C and 930° C (Table 2), and are significantly lower than those of host lavas which range between 950° C and 1150° C (Fig. 3). MIG mineral assemblages are similar to those reported by Dostal et al. (1980) from the Massif Central (France) (cf their assemblages B6, B7) and similarly imply 'intermediate' granulite facies conditions of Green and Ringwood (1967).

Relationship to host lavas

MIG xenoliths occur together with xenoliths of clearly automagmatic origin (i.e. cognate with host lavas), suggesting the possibility of a genetic link between them. In chemical composition, the MIG xenoliths do not plot entirely separately but strongly diverge from the fields of host lavas (Figs. 4–6). The clearest distinction, however, lies in their *isotopic* composition. A scattered plot that hardly touches the field of host lavas, results from the ε_{Nd} – $^{87}Sr/^{86}Sr$ data (Fig. 8), whereas the well-correlated trend for $\delta^{18}O$ – $^{87}Sr/^{86}Sr$ data leaves the field for the host lavas well to one side (Fig. 7). We need attach little significance to the fact that petrographically and chemically the compositions of MIG xenoliths and host lavas partly overlap, since both have a fairly indistinct, more or less arc-volcanic character. It is mainly the isotopic data therefore that distinguish the xenoliths, though their high-grade metamorphic textures, olivine-

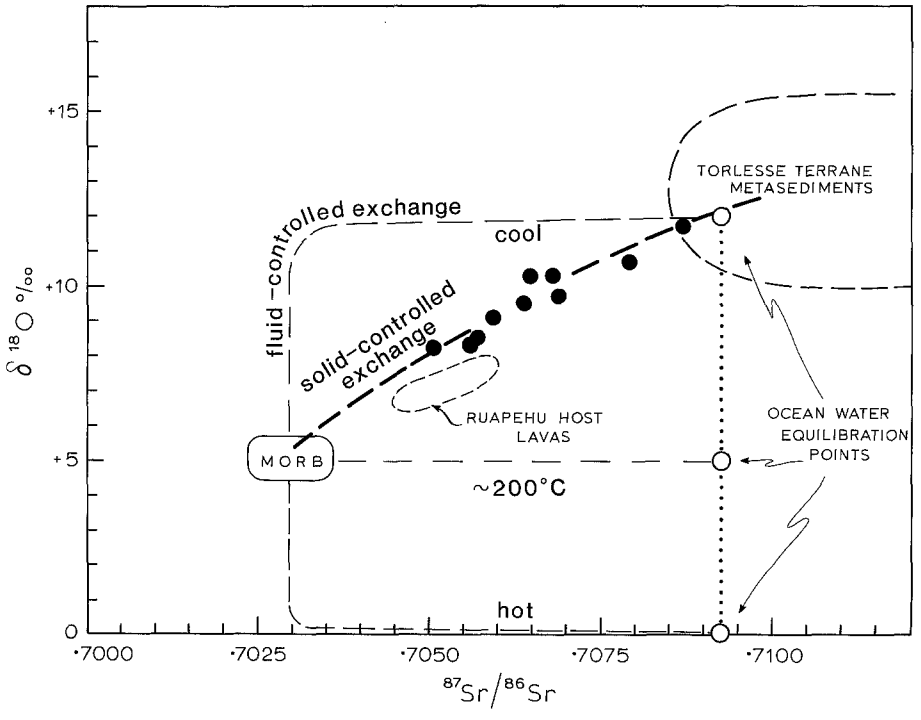

Fig. 7. $\delta^{18}O$ versus $^{87}Sr/^{86}Sr$ for MIG xenoliths. Torlesse and host lava $\delta^{18}O$ from Blattner & Reid (1982), and Blattner (unpublished data), $^{87}Sr/^{86}Sr$ from Graham (1985) and Graham and Hackett (1987). 2σ errors are approximately equal to the size of the data points. Equilibration pathways are drawn between MORB and ocean water for hot (~350° C) and cold (~100° C) fluid-controlled exchange using a zero-dimensional 'box' model. The actual data field could be ascribed to solid-buffered exchange, as well as to a model of fluid flow

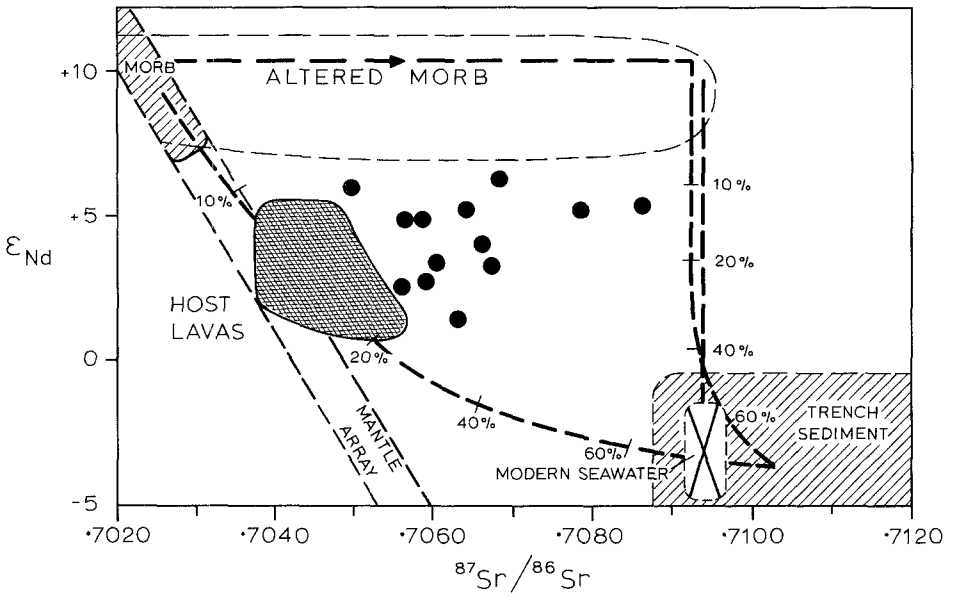

Fig. 8. ε_{Nd} versus $^{87}Sr/^{86}Sr$ for MIG xenoliths. Modern seawater composition from Piepgras and Wasserburg (1980) and De Paolo & Ingram (1985), MORB from McCulloch et al. (1981) and host lava compositions from Graham and Hackett (1987). *Arrows* indicate the effect of alteration of MORB by seawater, and *tick marks* show the effect of trench sediment addition

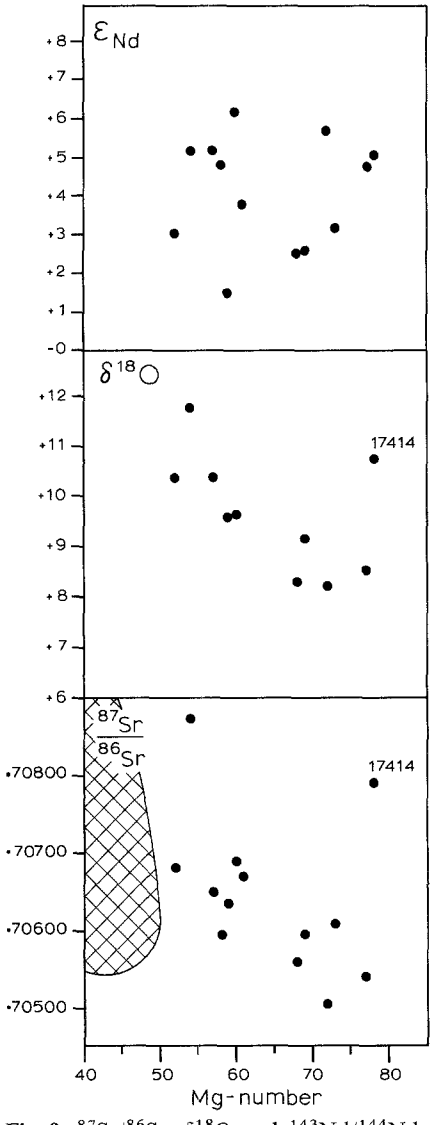

Fig. 9. $^{87}Sr/^{86}Sr$, $\delta^{18}O$ and $^{143}Nd/^{144}Nd$ versus Mg-number for MIG xenoliths. Field for other metasedimentary xenoliths (Graham 1987) is hashed. Note that the outlier on the $^{87}Sr/^{86}Sr$ and $\delta^{18}O$ plots (17414) lies on the $\delta^{18}O$ vs $^{87}Sr/^{86}Sr$ correlation (Fig. 7)

free (two pyroxene-plagioclase-ilmenite) mineral assemblages and relatively low LILE concentrations are also distinctive characteristics.

Origins

When considering the origin of the MIG xenoliths, we can either assume that the observed chemical and isotopic features are similar to those of the original protolith or, alternatively, that these features have been to some extent modified by metamorphism and metasomatism in the lower or middle crust, possibly during incorporation of the xenoliths in the host magma. The first situation (cf Dostal et al. 1980; Rudnick et al. 1986; Ruiz et al. 1988) allows us to search for protoliths from other settings in New Zealand or to postulate plausible, but presently unknown sources. The correlation between strontium and oxygen isotope ratios of the MIG xenoliths is an important consideration in that it, and indeed the range of each of the two isotope ratios, must be secondary since due to internal mixing (convection, diffusion) a magma could hardly display such properties originally. They must be a consequence of incomplete external mixing or exchange but this, too, could have taken place well in the past *or* as part of the more recent process responsible for producing the xenoliths.

In search of a known protolith

Metasedimentary basement. Basement rocks of the central North Island of New Zealand consist of the Mesozoic Torlesse terrane to the east and Manaia Hill Group (Waipapa) terrane to the west (Fig. 1). Each represents an accretionary prism complex dominated by turbidite sequences and with occasional metavolcanics and conglomerates. One possibility is that the MIG xenoliths are conglomerate clasts from these basement terranes. This is unlikely, however, because the basaltic-andesitic

chemistry of the xenoliths is inconsistent with the predominance of granitoid and felsic volcanic clasts found in the conglomerates (R.J. Korsch, personal communication, 1985). Alternatively, the xenoliths could be Torlesse terrane metavolcanics. Roser (1983) described 81 metabasites from North Island localities and showed that they are similar to ocean island basalts. Most have higher Ti and Zr contents than MIG xenoliths (Fig. 6) and their OIB trace element patterns are in contrast with the arc volcanic signatures of the xenoliths. In addition, these metabasites are, again, relatively rare and volumetrically restricted within the Torlesse terrane.

The highly refractory chemistries and low incompatible element contents of some of the MIG xenoliths may at first seem compatible with an origin as restites after partial melting of either Torlesse or Waipapa terrane greywacke. However, most of the MIG xenoliths analysed have Sr, Nd and oxygen isotope ratios outside the field for Torlesse terrane rocks (Figs. 7 and 8), Al_2O_3 and Sr contents lower than Waipapa terrane rocks and Cr, Ni contents many times higher than either. There is also a notable lack of refractory phases such as zircon, garnet and sphene which are fairly abundant in greywacke. Graham (1987) has shown that quartz-rich, feldspar-rich and spinel-rich xenoliths, which dominate the metamorphic xenolith suite from Ruapehu lavas (Table 1), have petrographic and chemical features much more consistent with such a restitic origin. Furthermore, these xenoliths fall in distinctly different fields from MIG xenoliths on most chemical and isotopic plots (cf. Figs. 4, 6 and 9).

Igneous basement. It is also possible that the MIG xenoliths originated from igneous rocks that might be located beneath the known Mesozoic sedimentary basement of the central North Island (either in place prior to deposition of Torlesse or Waipapa terranes or underthrust beneath them). Immobile elements Ti and Zr (Fig. 6) demonstrate compositional differences with two known igneous suites from the Eastern and Western Provinces of New Zealand, respectively (Korsch and Wellman 1988). Brook Street Arc volcanics which crop out in the northern and southern parts of the South Island, New Zealand (Coombs et al. 1976) are also typically tholeiitic but have much lower Zr contents (Williams and Smith 1979; Sivell and Rankin 1983). On the other hand, granulites of the Milford and Pembroke Formations of Fiordland, southernmost South Island, are higher in Ti, lower still in Zr and have substantially lower $^{87}Sr/^{86}Sr$ ratios (<0.7039, Blattner, in press; McCulloch et al. 1987). These geochemical differences, as well as the absence of any surface exposures or tectonic evidence for these southern terranes in the central North Island, also make them unattractive protoliths for the MIG xenoliths.

Possible unknown protoliths

Arc volcanic model. The isotopic correlation for MIG xenolith compositions shown in Fig. 7 could well be explained in terms of a solid-dominated mixing line between Torlesse terrane greywacke and MORB, suggesting a process of combined assimilation and fractional crystallisation (AFC) of arc-like basaltic rocks. However, the lack of a better $^{87}Sr/^{86}Sr$ vs ε_{Nd} correlation (Fig. 8) is a serious flaw in such a model since the low ε_{Nd} for Torlesse greywacke would not fit the process, and a required contaminant with both high and variable ε_{Nd} and high $^{87}Sr/^{86}Sr$ would be somewhat unusual and is not known in the New Zealand region. In addition, a simple model involving TVZ (or other North Island Late Cenozoic) magmas and Torlesse terrane basement would require a thermochemically impossible, up to 80% assimilation to explain the full Sr-O isotopic correlation. This would also be at odds with the relatively primitive chemical nature of most of the samples (i.e. low SiO_2, low LILE, high Mg number).

Altered oceanic crust model. In the absence of other plausible explanations, we look now at alternative mechanisms and protoliths. The isotopic features of MIG xenoliths could suggest hydrothermal alteration of ocean floor basalts and gabbros. Early work by McCulloch et al. (1981) emphasised an isothermal box model of ocean-water/rock exchange, which leads to strongly curved, L-shaped trajectories in the $\delta^{18}O$ vs $^{87}Sr/^{86}Sr$ field. Although the present correlation, shown in Fig. 7, shows very little curvature, it turns out that if the exchange is modelled by one-dimensional advective flow, sea floor hydrothermal alteration could well explain the relationship. The Sr isotopes indicate a sloped front, flattened by kinetic limitations of exchange, whereas the $\delta^{18}O$ tends to follow the temperature profile (Blattner and Lassey 1989). For oxygen, due to the larger effective porosity, the kinetic effects in the frontal zone have long passed the existing aquifer area and oxygen isotope compositions approach equilibrium, when Sr ratios are still far from it. Figure 10 shows a summary of this model and how a positive $\delta^{18}O$ vs $^{87}Sr/^{86}Sr$ correlation will

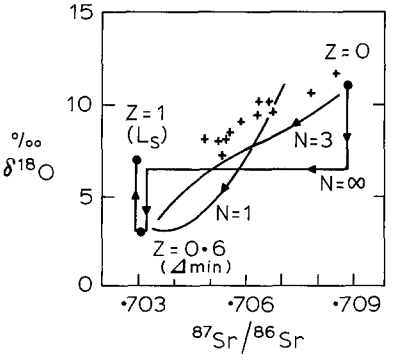

Fig. 10. $\delta^{18}O$ vs $^{87}Sr/^{86}Sr$ plot in a hypothetical sub-seafloor aquifer, showing predicted tracks for 'Damköhler numbers' $N=\infty$, 3, and 1. The length of the aquifer extends from the recharge at $Z=0$ to the discharge at $Z=1$, and the infiltration front has moved well past the discharge (aquifer filled ~ 15 times). Diagonal distributions such as found for the MIG-xenoliths (*crosses*) are highly likely for expected N values near unity. Xenoliths would come from the descending part of the system, before reaching maximum temperature at $Z \simeq 0.6$ (see also Blattner and Lassey 1989)

arise for very reasonable kinetics. The data of McCulloch et al. (1981, Fig. 11) fit a one-dimensional model equally well. We note, however, that the MIG xenolith samples would represent only the initial branch of the flow path, namely that of descending solutions to ~250° C, and this model could finally be confirmed only by the discovery of xenoliths with lower $\delta^{18}O$ values ($\lesssim 5‰$).

Despite the relatively large ranges of both the Sr and Nd isotopic ratios of the MIG xenolith suite, there is no correlation between ε_{Nd} and $^{87}Sr/^{86}Sr$. Figure 8 shows a pattern similar to that predicted for mixtures of oceanic crust, altered hydrothermally by interaction with sea water, and trench sediment (added 'chemically' by fluid exchange) (after McCulloch and Perfit 1981). Assuming that TVZ trench sediments have Nd-Sr isotopic compositions similar to Torlesse terrane sediments (±TVZ rhyolite) then mixtures of sediment with altered oceanic crust (i.e. altered MORB) would define a roughly triangular area as shown (see also McCulloch et al. 1981). Figure 8 thus suggests a two-stage process by which the observed isotopic data distribution of MIG xenoliths could come about. First, a seafloor geothermal system could create the correlation between Sr and $\delta^{18}O$ (Fig. 7) and second, admixture of trench sediment during subduction could lower, and to some extent scatter, the Sr and Nd isotopic compositions and could also provide the characteristic arc-type trace element patterns (Fig. 5). Because of the extremely low ($<10^{-6}$) Nd/Sr ratio of seawater, the first stage would leave the MORB ε_{Nd} values virtually unchanged (e.g. O'Nions et al. 1978), whereas the second stage should decrease ε_{Nd} to between about +1 and +6, assuming approximately 10 to 20% admixture of sediment. The effect of sediment admixture on a pre-existing positive $\delta^{18}O - ^{87}Sr/^{86}Sr$ correlation would be to raise slightly the values at the low end and leave the upper (and previously most altered) end almost unchanged, so that the correlation of Figs. 7 and 8 would commence at somewhat higher values and appear slightly squashed at the low end. Because of the relatively high Nd but low Sr contents of sediments in relation to MORB, and therefore small requirements of admixture to achieve the ε_{Nd} shift of Fig. 8, the correlation between O- and Sr-isotopes would not be strongly affected.

Hence, a possible explanation for the MIG xenolith suite is that they comprise altered oceanic crust with a small component of trench sediment added. Whilst a variable addition of sediment would account for the Nd isotopic systematics, sediment addition seems necessary also because an enriched mantle source for Tonga-Kermadec-TVZ oceanic crust is not predicted (Cole 1982; Ewart and Hawkesworth 1987). There is increasing evidence that significant amounts of trench sediment are currently being subducted at oceanic and continental arc systems, accounting for many of their geochemical and isotopic characteristics (Karig and Kay 1981; O'Nions 1984; Kay and Kay 1988).

No satisfactory explanation has been found for the apparent negative correlations between $^{87}Sr/^{86}Sr$ and $\delta^{18}O$ and Mg number (Fig. 9), but in this model one possibility is that the high Mg number MIG xenoliths have been less exchanged due to their coarser grain size or due to exposure to less fluid in a marginal (lower?) part of the aquifer.

If the MIG xenoliths do represent descendants of altered oceanic crust, then two possible scenarios could explain their occurrence in Ruapehu lavas. In the first, melting and dismembering of the presently subducting slab beneath the TVZ might occur during descent into the mantle. Liquids produced by this melting pass into the mantle wedge, and there mix with peridotitic partial melts, ultimately to yield basaltic and andesitic magmas (Wyllie 1984). The MIG xenoliths would have to represent fragments of slab restite that became entrained in these magmas and were carried to the surface by them. High-pressure minerals may have been removed in the xenoliths, through re-equilibration in lower-crustal magma chambers (Graham and Hackett 1987). Although it is difficult to visualise a mechanism by which the xenoliths make their ascent through the mantle wedge, it might be that small volumes of slab melt promote the formation of diapirs close to the slab surface and that these rise through the wedge, carrying small fragments of dismembered slab residue with them.

Such difficulties could be avoided by postulating a MIG protolith consisting of older altered oceanic crust, underthrust beneath Ruapehu Mesozoic basement. Partial melting within or above the mantle wedge would be caused by high heat flow due to ascending mantle-derived magmas, and residues of this melting could become entrained in magmas pooling in the lower crust. An underthrust protogranulite could be of sufficiently recent origin still to be associated with current TVZ subduction activity, but due to decay of unrelated amounts of Rb, a pre-existing $^{87}Sr/^{86}Sr$ vs $\delta^{18}O$ correlation would not be preserved if the protolith were more than a few hundred million years old. Underthrusting of oceanic crust due to burial and downwarping of the overlying arc volcanics (Kay and Kay 1986) has been suggested for the Aleutians where it may have produced a significant part of the arc column (Kay and Kay 1985).

Lower crust hydrothermal exchange

An alternative to the 'ocean floor' model explanation for the O-Sr isotope correlation has the MIG xenoliths modified by rock-controlled intracrustal isotope exchange between granulites of unknown lower crustal origin (with somewhat scattered ε_{Nd} values) and Torlesse terrane basement, whereby hydrothermal fluid would have acted as a medium of transport only. The actual isotope exchange would hence be controlled by the solid rock participants and intermediate compositions would lie on the nearly straight line of Fig. 7. The locus for such a process could be the vicinity of magma chambers at the contact between Torlesse greywacke cover and a granulite basement. Even if the magma was itself volatile undersaturated, its soaking up of fluid from the wall rocks could be sufficiently complex in detail to allow isotope exchange within limited volumes. The timing of

the exchange is still open, namely either before or during granulite metamorphism, or in the present genetic cycle before incorporation as xenoliths. Plagioclase-pyroxene pairs for xenoliths 17424 and 17449 give equilibrium $\delta^{18}O$ values consistent with granulite facies or magmatic temperatures (Table 3; footnote). They are consistent, as in the ocean floor option, with a $\delta^{18}O - {}^{87}Sr/{}^{86}Sr$ correlation older than the granulite facies metamorphism, but with magmatic/hydrothermal alteration taking place *after* the metamorphism only if temperatures were high enough ($\geq 500°$ C).

This final model of intracrustal exchange effectively sidesteps the issues of the primary origin of the xenoliths, relying merely on what happens to be present in the crust below Mt Ruapehu. Many igneous protolith comprising volcanics and cumulates could be suitable, and hydrothermal as well as greywacke exchange in the vicinity of the host magma could mean that granulites become affected while being approached by the magma, before entering it as xenoliths, so that the $\delta^{18}O$ vs $^{87}Sr/^{86}Sr$ correlation would not require to be an original characteristic of the granulite.

Conclusions

The MIG xenoliths represent fragments of the lower arc crust beneath the Taupo Volcanic Zone and provide rare evidence for the nature of the basement beneath the Mesozoic greywacke in the Central North Island of New Zealand. Several origins are possible, the most likely being: (1) fragments of altered oceanic crust of past or present regimes of subduction and (2) unknown metaigneous rocks, isotopically altered by lower crustal fluids circulating into or from the overlying metasedimentary basement. Whilst the altered ocean crust model has many attractive features, we find it impossible to reject the less complicated lower crustal alteration model. As yet, neither model explains all the features of MIG xenoliths though this may be put down to the complexities of, and lack of constraints for, xenolith genesis in general. We note that oxygen isotopes are used in few studies of rocks of lower crustal origin despite their potentially wide spectrum of values and the likelihood that hydrothermal exchange has played a role at some stage of petrogenesis.

Compositionally, the protolith of the MIG xenoliths appears to be a possible source rock for the voluminous rhyolitic magmas which occur in the main part of the Taupo Volcanic Zone. A few percent of interstitial glass in sample 17422 is of rhyolitic composition and might represent a residue of partial melt. We hope that further investigations of this possibility can follow.

Acknowledgements. We thank Dr. W.R. Hackett for providing most of the samples and for early suggestions and interpretation. Thanks are extended also to Drs J.A. Gamble, R.J. Arculus and J.D. Myers for perceptive and helpful reviews of the manuscript, to Mrs Anne Hepenstall for word processing and Mrs Margaret McDonald for figure drafting.

References

Adams CJD (1975) Discovery of Precambrian rocks in New Zealand: age relations of the Greenland Group and Constant Gneiss, West Coast, South Island. Earth Planet Sci Lett 28:98–104

Arculus RJ (1986) Arc magmatism – an unresolved problem of sources, material fluxes, tectonic evolution and thermochemical regions of subduction zones. In: Nasu N (ed) Formation of active ocean margins. Terra Scientific Pub, Tokyo/Kluwer, Dordrecht, pp 367–397

Blattner P (in press) The North Fiordland transcurrent convergence. NZ J Geol Geophys

Blattner P, Lassey KR (1989) Stable-isotope exchange fronts, Damköhler numbers, and fluid to rock ratio. Chem Geol 78:381–392

Blattner P, Reid F (1982) The origin of lavas and ignimbrites of the Taupo Volcanic Zone, New Zealand, in the light of oxygen isotope data. Geochim Cosmochim Acta 46:1417–1429

Cole JW (1979) Structure, petrology and genesis of Cenozoic Volcanism, Taupo Volcanic Zone, New Zealand – a review. NZ J Geol Geophys 22:631–657

Cole JW (1982) Tonga-Kermadec-New Zealand. In: Thorpe RS (ed) Andesites. Wiley, Chichester New York Brisbane Toronto Singapore, pp 245–258

Cole JW, Lewis KB (1982) Evolution of the Taupo-Hikurangi subduction system. Tectonophysics 72:1–21

Conrad WK, Kay RW (1984) Ultramafic and mafic inclusions from Adak Island: crystallisation hisotry, and implications for the nature of primary magmas and crustal evolution in the Aleutian Arc. J Petrol 25:88–125

Conrad WK, Nicholls IA, Wall VJ (1988) Water-saturated and under-saturated melting of metaluminous and peraluminous crustal compositions at 10 kb: evidence for the origin of silicic magmas in the Taupo Volcanic Zone, New Zealand, and other occurrences. J Petrol 29:765–803

Coombs DS, Landis CA, Norris RJ, Sinton JM, Borns DJ, Craw D (1976) The Dun Mountain Ophiolite Belt, New Zealand, its tectonic setting, constitution, and origin, with special reference to the southern portion. Am J Sci 276:561–603

DePaolo DJ, Ingram BL (1985) High resolution stratigraphy with strontium isotopes. Science 227:938–940

Dostal J, Dupuy C, Leyreloup A (1980) Geochemistry and petrology of meta-igneous granulite xenoliths in neogene volcanic rocks of the Massif Central, France – Implications for the lower crust. Earth Planet Sci Lett 50:31–40

Ewart A, Hawkesworth CJ (1987) The Pleistocene-Recent Tonga-Kermadec Lavas Interpretation of New Isotopic and Rare Earth Data in Terms of a Depleted Mantle Source Model. J Petrol 28:495–530

Gill JB (1981) Orogenic Andesites and Plate Tectonics. Springer-Verlag, Berlin

Graham IJ (1985) Rb-Sr geochronology and geochemistry of Torlesse metasediments from the Central North Island, New Zealand. Chem Geol (Isotope Geoscience Section) 52:317–331

Graham IJ (1986) The Rb-Sr system. DSIR, (NZ) Internal publication. INS-M-65

Graham IJ (1987) Petrochemistry and origin of metasedimentary xenoliths in lavas from Tongariro Volcanic Centre. NZ J Geol Geophys 30:139–157

Graham IJ, Hackett WR (1987) Petrology of calc-alkaline lavas from Ruapehu Volcano and related vents, Taupo Volcanic Zone, New Zealand. J Petrol 29:531–567

Grapes R, Palmer K (1984) Magma type and tectonic setting of metabasites, Southern Alps, New Zealand, using immobile elements. NZ J Geol Geophys 27:21–26

Green DH, Ringwood AE (1967) An experimental investigation of the gabbro to eclogite transformation and its petrological applications. Geochim Cosmochim Acta 31:767–833

Hildreth W, Moorbath S (1988) Crustal contributions to arc magmatism in the Andes of Central Chile. Contrib Mineral Petrol 98:455–489

Karig DE, Kay RW (1981) Fate of sediments on the descending plate at convergent plate margins. Philos Trans Soc London A301:233–251

Kay RW, Kay SM (1986) Petrology and geochemistry of the continental crust. In: Dawson JB, Carswell DA, Hall J, Wedepohl KH (eds) The nature of the lower continental crust. Geological Society Special publication No 24, pp 147–159

Kay RW, Kay SM (1988) Crustal recycling and the Aleutian arc. Geochim Cosmochim Acta 52:1351–1359

Kay SM, Kay RW (1985) Role of crystal cumulates and the oceanic crust in the formation of the lower crust of the Aleutian Arc. Geology 13:461–464

Korsch RJ, Wellman HW (1988) The geological evolution of New Zealand and the New Zealand region. In: Nairn AEM, Stehli FC, Uyeda S (eds) The ocean basins and margins, Vol. 7: The Pacific Ocean, Plenum, New York, pp 411–482

Lindsley DJ (1983) Pyroxene thermometry. Amer Mineral 68:477–493

McCulloch MT, Bradshaw JY, Taylor SR (1987) Sm-Nd and Rb-Sr isotopic and geochemical systematics in Phanerozoic granulites from Fiordland, Southwest New Zealand. Contrib Mineral Petrol 97:183–195

McCulloch MT, Gregory RT, Wasserburg GJ, Taylor HP Jr (1981) Sm-Nd, Rb-Sr and $^{18}O/^{16}O$ isotopic systematics in an oceani crustal section: evidence from the Samail Ophiolite. J Geophys Res 86(B4):2721–2735

McCulloch MT, Perfit MR (1981) $^{143}Nd/^{144}Nd$, $^{87}Sr/^{86}Sr$ and trace element constraints on the petrogenesis of Aleutian Island arc magmas. Earth Planet Sci Lett 56:167–179

McDonough WF, McCulloch MT, Sun SS (1985) Isotopic and geochemical systematics of Tertiary-Recent basalts from southeastern Australia and implications for the evolution of the subcontinental lithosphere. Geochim Cosmochim Acta 49:2051–2068

O'Nions RK (1984) Isotopic abundances relevant to the identification of magama sources. Philos Trans R Soc London A310:591–603

O'Nions RK, Carter SR, Cohen RS, Evensen NM, Hamilton PJ (1978) Pb, Nd and Sr isotopes in Oceanic ferromanganese deposits and ocean floor basalts. Nature (London) 273:435–438

Pearce JA (1982) Trace element characteristics of lavas from destructive plate boundaries. In: Thorpe RS (ed) Andesites. Wiley, Chichester New York Brisbane Toronto Singapore, pp 525–548

Pearce JA, Cann JR (1973) Tectonic setting of basic volcanic rocks determined using trace element analyses. Earth Planet Sci Lett 19:290–300

Piepgras DJ, Wasserburg CJ (1980) Neodymium isotopic variations in seawater. Earth Planet Sci Lett 50:128–138

Reid F (1983) Origin of rhyolitic rocks of the Taupo Volcanic Zone, New Zealand. J Volcanol Geophys Res 15:315–398

Reyners M (1980) A microearthquake study of the plate boundary, North Island, New Zealand. Geophys J R Astron Soc 63:1–22

Roser BP (1983) Comparative studies of copper and manganese mineralisation in the Torlesse, Waipapa and Haast Schist terranes, NZ. Unpublished PhD thesis, Victoria University of Wellington, NZ

Rudnick RL, McLennan SM, Taylor SR (1985) Large ion lithophile elements in rocks from high-pressure granulite-facies terranes. Geochim Cosmochim Acta 49:1645–1655

Rudnick RL, McDonough WF, McCulloch MT, Taylor SR (1986) Lower crustal xenoliths from Queensland, Australia: Evidence for deep crustal assimilation and fractionation of continental basalts. Geochim Cosmochim Acta 50:1099–1115

Ruiz J, Patchett PJ, Arculus RJ (1988) Nd-Sr isotope composition of lower crustal xenoliths – Evidence for the origin of mid-Tertiary felsic volcanics in Mexico. Contrib Mineral Petrol 99:36–43

Sivell W, Rankin P (1983) Arc-tholeiite and ultramafic cumulate, Brook Street volcanics, west D'Urville Island, New Zealand. NZ J Geol Geophys 26:239–258

Stern TA, Davey RJ (1987) A seismic investigation of the crustal and upper mantle structure within the Central Volcanic Region of New Zealand. NZ J Geol Geophys 30:217–231

Williams JG, Smith IEM (1979) Geochemical evidence for paired arcs in the Permian volcanics of southern New Zealand. Contrib Mineral Petrol 68:285–291

Winkler HGF (1979) Petrogenesis of metamorphic rocks, 3rd edn. Springer, Berlin Heidelberg New York, p 320

Wyllie PJ (1984) Constraints imposed by experimental petrology on possible and impossible magma sources and products. Philos Trans R Soc London A310:439–456

Editorial responsibility: T. Grove